INTERNATIONAL JOURNAL OF AUTOMOTIVE AND MECHANICAL ENGINEERING
ISSN: 2229-8649 e-ISSN: 2180-1606
VOL. 22, ISSUE 1, 2025, 12035 – 12047
DOI: https://doi.org/10.15282/ijame.22.1.2025.7.0924

RESEARCH ARTICLE

Optimization of 3D Printing Parameters for Enhanced PLA Tensile Strength Using the Taguchi Method

Rolland Darin Khalifah Mahameru, Ahmad Khairul Faizin*, M. Danny Pratama Lamura, Wahyu Dwi Lestari

Mechanical Engineering Departement, Universitas Pembangunan Nasional "Veteran" of East Java, Surabaya, Indonesia

ABSTRACT – Fused Deposition Modeling (FDM) has significantly advanced in the additive manufacturing of complex geometrical and customized parts, particularly for thermoplastics like Polylactic Acid (PLA). The present study aimed to optimize FDM process parameters to improve the tensile strength of 3D-printed PLA, a crucial mechanical property for various applications. The Taguchi method was employed to systematically and effectively analyze the effects of six key process parameters: nozzle temperature, printing speed, layer thickness, infill density, infill pattern, and orientation. The analysis revealed that among these parameters, only nozzle temperature and infill density had a significant impact on tensile strength, as demonstrated by the variance analysis. By optimizing these critical parameters, the tensile strength of the printed PLA parts was improved from the previously reported 35 MPa to 40 MPa, representing a notable enhancement. Additionally, a linear regression-based empirical model was developed, achieving an R-squared value of 89.2%, enabling accurate prediction of tensile strength for given process parameter values. These findings provide a vital foundation for enhancing the mechanical performance of FDM-printed PLA components. They are particularly relevant for applications across industries requiring high-strength materials, further solidifying the potential of FDM in advanced manufacturing scenarios.

ARTICLE HISTORY
Received : 29th Aug. 2024
Revised : 21st Oct. 2024
Accepted : 27th Nov. 2024
Published : 20th Feb. 2025

KEYWORDS
Additive manufacturing
Fused Deposition Modelling
Polylactic acid
Tensile strength
Taguchi method
Process optimization

1. INTRODUCTION

Additive manufacturing is the technique of 3D printing, where products are built with special attention in layer-by-layer construction, enabling precision and design flexibility previously unattainable and making complex geometries possible that could hardly have been achieved, if at all, by conventional methods of manufacturing [1, 2]. Advances in additive manufacturing (AM) technology have massively affected different industries due to a shift in design flexibility and economic advantage. It allows the rapid prototyping of mechanical components; hence, it allows for fast turnover of prototypes at low quantities, a feature useful in industries like automotive, aerospace, and medical devices [3-5]. Recent studies are delving deeper into the potential uses and diverse materials associated with AM. Researchers are not only broadening the scope of its applications but are also discovering innovative material combinations that enhance performance and functionality. These advancements underscore the increasing significance of AM in the manufacturing sector, as it continues to revolutionize traditional production methods and pave the way for more efficient, customized, and sustainable solutions [6].

There are several different types of additive manufacturing techniques, each suited to a different material and application. These include Fused Deposition Modelling (FDM), Fused Filament Fabrication (FFF), Stereolithography (SLA), and Selective Laser Sintering (SLS). Each of these methods has specific advantages, depending on the application. FFF is considered the most simple, low-cost, and versatile technique; hence, it is very popular among both hobbyists and professionals. FFF stands out for its ease of use, the variety of raw materials that can be used in the printing process, its adaptability to different designs, and its capability to support continuous production runs, especially in prototyping and small-scale manufacturing [7, 8].

Polylactic Acid (PLA) is one of the most commonly used materials in FFF printing. Its availability is significantly supported by its excellent processability, biocompatibility, and bio-friendly features due to its biodegradable nature. PLA is manufactured from renewable feedstocks such as corn starch or sugarcane, which further adds to its popularity as a renewable alternative to petroleum-based plastics. PLA, on the other hand, despite the many benefits it provides in terms of mechanical and thermal properties, has some shortcomings that cannot suffice in some high-performance usages. [9, 10]. Hence, many studies have focused on the development of PLA-based composites with improved properties.

Research into the addition of various reinforcements to the PLA matrix includes natural fibers such as cellulose, synthetic fibers like carbon or glass, and even metals and ceramics in an attempt to improve its mechanical strength, thermal stability, and overall durability. The addition of reinforcement in PLA is meant to overcome the intrinsic weaknesses in PLA and further extend the application of PLA in a wide variety of applications where higher strength, rigidity, or wear and impact resistance is needed [11-13]. Surprisingly, these new PLA composite classes have brought

*CORRESPONDING AUTHOR | Ahmad Khairul Faizin | ✉ ahmad.khairul.tm@upnjatim.ac.id

about a whole new dimension of challenges, especially in the functional and mechanical property optimization compromises related to FFF printing.

The effects of temperature, printing speed, layer height, and infill density are among the important parameters that need to be understood in order to obtain optimum mechanical performance in FFF-printed PLA composites. All these parameters must be controlled with care and optimized so that the composite material performs in the manner it is supposed to in its specific application. For example, the temperature of printing and the rate of cooling can seriously affect the bonding between layers, which is the key to the structural integrity of the printed part. Similarly, the orientation of fibers in the PLA matrix during printing can influence the anisotropy of the material and further its mechanical properties.

The basic process parameters of FFF include nozzle temperature, fill density, layer thickness, and print speed, which have a great impact on the quality and performance of the manufactured parts. These parameters directly affect mechanical properties, including tensile strength and surface finish [14-16]. It basically denotes that the ability to optimize such parameters in a way to balance the mechanical performance onboard with resource efficiency is important, especially when the going concern is cost control. Single-objective optimization, through ANOVA, will be one of the best options to determine the optimal printing parameters since it simplifies the analysis and narrows the investigation scope to key performance metrics such as tensile strength or elasticity [17].

Single-objective optimization, in particular, if approached by the ANOVA method, can be done in a more systematic and efficient way of testing the impact caused by different printing parameters. ANOVA is preferred here because it makes the analysis easier by considering one response variable at a time. This clarity is especially welcome when put in the context of multi-objective optimization methods, which, although comprehensive, can get quite complex and may introduce uncertainties owing to the need to balance several conflicting objectives. In particular, a clear focus on one key performance metric, such as tensile strength or elasticity, enables the researchers to identify an optimum set of printing parameters with more ease, leading to more reliable and reproducible results [18].

The effectiveness of ANOVA in the optimization of FFF printing parameters has been well documented. For example, several studies have used the Taguchi method in conjunction with ANOVA to investigate and optimize the effects of various FFF parameters on the mechanical properties of printed components. John et al. [19], for instance, studied the influence of nozzle diameter, strain rate, and geometric patterns on the mechanical properties of PLA samples. According to their analysis, nozzle diameter and geometric pattern account for 48.99% and 40.78% of the overall variation in mechanical attributes, respectively. This, therefore, presents an avenue for focused changes that will have the desired outcomes in printed products. Kumar and Singh et al. [20] applied a Taguchi-based DoE to optimize the layer height and infill pattern for PLA surgical equipment produced via FFF. In the process of optimization, they reached a tensile strength of 42.6 MPa and an elasticity modulus of 32.74 MPa, showing that tight control of the FFF parameters can greatly improve the mechanical performance of the product.

Ranjan et al.[21] further investigated the optimization of print speed, layer height, and deposition rate for maximum tensile strength with minimum surface roughness. Their findings underlined the fact that such parameters may be critical in achieving the highest quality in FFF prints, where the correct combination can yield superior mechanical properties and surface finishes. Similarly, Farayibi et al. [22] also used the DoE method to find the optimal setting for extrusion temperature, layer thickness, and infill density to produce a material tensile strength of 30.02 MPa and an impact strength of 4.20 J, showing how important these factors are in determining the mechanical properties of FFF printed part. Gebrehiwot et al. [23] have also shown the efficiency of using DoE for the optimization of parameters in FFF and Marble-PLA, which presents a series of optimal values for layer height, print speed, and cell geometry. Their work also enforces the previous assertion of the need for optimization of these parameters to achieve the desired mechanical and aesthetic characteristics of printed components. Chinchanikar et al.[24] also applied DoE for the optimization of some of the most critical FFF parameters related to print speed, extrusion temperature, layer thickness, and infill density, and were able to identify the optimal setting for PLA parts. Their finding thus evidences the crucial role that careful control and optimization of FFF operating parameters can play in enhancing not only the quality but even the performance of 3D printed parts.

The FFF process is optimized in this study using a PLA composite material by the Taguchi method and ANOVA, having a single objective: tensile strength of the material. Therefore, the printing parameters considered are nozzle temperature, infill density, infill pattern, layer thickness, printing speed, and orientation. Each parameter's effect on process performance will be investigated based on the Taguchi L27 experimental design. The Taguchi method helps in finding the most influencing parameters and their optimum combinations. ANOVA is used to confirm the effects of parameters on performances. Experiments are made for validation to confirm the results of optimization. Though there are many studies that have optimized the mechanical properties of PLA through FFF and supported by ANOVA, most of them are based on a few process parameters or some specific reinforcement materials. This work tries to fill this gap by investigating six critical parameters using a robust Taguchi-based experiment design. Our work presents a new approach to optimize PLA composites by integrating these parameters, collectively giving an enhanced tensile strength, which has also not been addressed in depth in current literature.

2. MATERIALS AND METHODS

In the Design of Experiments (DoE), focusing solely on the main effects allows for a more straightforward analysis, but this approach inherently limits the depth of exploration, particularly when it comes to understanding the interactions between different factors. While an analysis of the main effects facilitates singling out which factors influence a response variable most significantly, its major weakness lies in sacrificing an examination of the interaction between main factors that might show effects as interesting, if not more interesting. This is a very common trade-off since complex systems often require such a large number of experiments and resource budgets that running a full factorial design may be impracticable. If one considers only the main effects, there are a total of 10 DoF in the experiment. Since each DoF is associated with a main effect, the DoF for each of the main effects is one less than the number of levels for that factor. If any factor has three levels, its corresponding DoF would be two. This calculation becomes necessary for determining the appropriate experimental design since this will directly influence the orthogonal array to be used. In this case, an orthogonal array like L27 (3^6), as indicated in Table 3, is quite applicable for 27 experimental runs with six factors at three levels each. The L27 array provides a symmetrical and comprehensive assessment of the main effects while minimizing confounding, meaning that the effects of two or more factors cannot be distinguished.

This is not an arbitrary choice but is rooted in the principles of statistical efficiency and experimental design. The chosen L27 orthogonal array tries to optimize the conflict between adequate exploration of the factor space and the practical limitation in the number of experiments that could be done. The use of the L27 array ensures that the effects of any factors are unbiased during estimation, allowing accurate and reliable conclusions to be drawn through this approach. Also, with an orthogonal array, such effects are much better supported and retained, which can cause lesser risks pertaining to multicollinearity, which, when internal correlation happens among a pair or more predictor variables, may complicate accurate effect estimates. Confounding minimization is key for the reliability of the experimental results using DoE. In some cases, confounding occurs because the effect of one factor becomes combined with that of another factor, and in turn, makes it difficult to draw a correct conclusion on how each factor affects a response variable. This may be minimized through an intelligent choice of design for the experiment, such as the L27 orthogonal array, in order to improve the accuracy and reliability of a research study. Confounding is important in experiments in which the response variable is sensitive to changes in the experimental conditions. Even little confounding may cause substantial errors in interpretation.

L27 array is good for balancing the design in both statistical analysis and experimental design, as it is in the literature. Accommodating 27 runs provides data with which main effects can be estimated very well with precision, although offering some idea on interaction effects when compared with a full factorial, yet in less detail. This balance of simplicity and thoroughness makes the L27 array an attractive option in experiments where the main goal is to identify the most critical factors affecting the response variable without delving deeply into the complexities of factor interactions.

2.1 Material and Specifications

PLA was the filament used to prepare the tensile specimens. Commercially available from Filament Company of 1.75 mm diameter (Shenzhen, China), some technical specifications of composite PLA are given in Table 1. Tensile test samples were produced using the Flashforger Guider IIs FFF technology-based 3D printer, in Beijing, China. The tensile test specimens are designed as per the ASTM-D638 Type IV standards, represented in Table 1 and modeled using CAD software with Solidworks 2020. Once the model is sliced through the Flashprint slicing software, g-code is generated. G-code is a kind of programming language. It is a set of commands telling a 3D printer how to print objects. Examples of information that G-code conveys are how the printer moves, at what speed, and the required temperature of the extruder. Sliced code is a code comprising directives along with both variable and constant parameters necessary for the slicing program. These are illustrated in Table 2 below.

Table 1 presents the key physical and mechanical properties of PLA filament, including tensile strength, elongation at break, density, melting temperature, and glass transition temperature. These properties are critical for understanding the performance of PLA in additive manufacturing applications.

Table 1. Properties of Polylactic Acid (PLA) filament

Property	Value	Units
Density	1.3	Kg / m^{-3}
Elongation at break	6	%
Ultimate tensile strength	50	MPa
Tensile modulus	3.5	GPa
Rockwell hardness	80	Hr
Melting temperature (Tm)	175 - 185	C^o
Glass transition temperature (Tg)	55 - 70	C^o

The variable parameters set for the 3D printing process through FlashPrint software in the case of PLA are noted in Table 2: nozzle temperature (A), infill pattern (B), layer thickness (C), printing speed (D), infill pattern (E), and orientation (F). These parameters have been manipulated systematically to evaluate their influence on the tensile strength of the printed components.

Table 2. Variable parameters used in Flashprint software

No.	Process Parameters	Levels			Units
		1	2	3	
1.	Nozzle Temperature (A)	190	200	210	°C
2.	Infill Density (B)	80	90	100	%
3.	Layer Thickness (C)	0.15	0.2	0.25	mm
4.	Printing Speed (D)	70	80	90	mm / s
5.	Infill Pattern (E)	Line	Triangle	Hexagon	-
6.	Orientation (F)	0	15	30	-

The following Taguchi L27 orthogonal array (Table 3) was used for the design of the experiment, showing various combinations of the six process parameters: nozzle temperature, infill density, infill pattern, layer thickness, printing speed, and orientation, along with levels. This will systematically allow the study of multiple factors affecting the tensile strength of 3D-printed PLA.

Table 3. Taguchi L_{27} Orthogonal array for design of experiments (DoE)

Sample	Nozzle Temperature (A)	Infill Density (B)	Layer Thickness (C)	Printing Speed (D)	Infill Pattern (E)	Orientation (F)
1.	1	1	1	1	1	1
2.	1	1	1	1	2	2
3.	1	1	1	1	3	3
4.	1	2	2	2	1	1
5.	1	2	2	2	2	2
6.	1	2	2	2	3	3
7.	1	3	3	3	1	1
8.	1	3	3	3	2	2
9.	1	3	3	3	3	3
10.	2	1	2	3	1	2
11.	2	1	2	3	2	3
12.	2	1	2	3	3	1
13.	2	2	3	1	1	2
14.	2	2	3	1	2	3
15.	2	2	3	1	3	1
16.	2	3	1	2	1	2
17.	2	3	1	2	2	3
18.	2	3	1	2	3	1
19.	3	1	3	2	1	3
20.	3	1	3	2	2	1
21.	3	1	3	2	3	2
22.	3	2	1	3	1	3
23.	3	2	1	3	2	1
24.	3	2	1	3	3	2
25.	3	3	2	1	1	3
26.	3	3	2	1	2	1
27.	3	3	2	1	3	2

Figure 1 is an all-inclusive representation showing the equipment and methodologies adopted in experiments, right from the fabrication of the specimen to the analyses of the fractured specimens obtained from tensile tests. Each level of this process is carefully designed and implemented to ensure that the experimental results attain both precision and reliability, thus offering a sound understanding of the material properties under investigation.

The experimental process starts with the precise determination of fabrication time using Flashprint slicing software. This software is central in the planning phase, as it allows researchers to generate accurate estimates of time for each stage of the production process. The estimates are not just theoretical but are rigorously compared with actual production times during FFF to ensure that they are consistent and reliable. It is in such comparisons where the details are provided to identify not only the differences, if any, between the predicted and actual on-site times but also how such variability within these can be minimized. This is a key process for achieving consistent production. In this way, the subsequent mechanical testing would also become more reliable, as errors or inconsistencies would be minimized, preventing biased results.

Precise measurement of material consumption is one of the most important aspects of the experimental process. Each manufactured specimen is weighed with a high degree of accuracy using a high-precision scale with an accuracy of ±0.01 grams. This step is very important for a number of reasons. First, it allows for the precise calculation of material usage, which is crucial in analyzing efficiency in the manufacturing process. By knowing precisely how much material is being consumed, a researcher can optimize the process to minimize waste and cut costs in order to give an eco-friendly touch. This secondly furnishes data by which to further refine the process of fabrication. For example, specific phases of the production process may be overly wasteful and could use refinement in material consumption without compromising product quality.

The tensile testing in the experiment is conducted with a specially fabricated Zwick/Roell testing machine with a capacity of 2 kN, designed to accommodate the material's low tensile strength. The selection of this special equipment was particularly crucial for making the conditions perfect according to the properties studied in materials. The machine can provide accurate control of the application of force, ensuring that the same amount of stress is applied in all tests. The tensile testing speed is set at 50 mm/min, which optimizes the measurement of material response during loading. Furthermore, the machine can provide very accurate elongation measurements and fracture points in detail, which are integral parts of a detailed analysis of the mechanical properties of materials. This is the only way to get reliable and reproducible results, which is important for meaningful conclusions from the data.

Moreover, the integration of these high-precision tools and the controlled testing environment greatly enhances the quality of the experimental data. This data quality is essential, forming the foundation of the entire analysis process. Reliable data supports robust statistical analysis, enabling researchers to derive well-founded conclusions. The rigorous methodology employed throughout ensures that the findings are valid and align with existing literature. This is especially critical in material science and engineering, where accuracy and reproducibility are necessary for experimental results to be deemed trustworthy.

The use of precise measurement tools and strict testing protocols significantly increases the potential for applying these findings in real-world scenarios. For example, the research insights may guide the development of new materials or enhance the performance of existing ones, fostering innovations in manufacturing. By reliably measuring and analyzing material properties in controlled environments, this work lays a solid foundation for future research and development, promising progress in both academic and industrial fields.

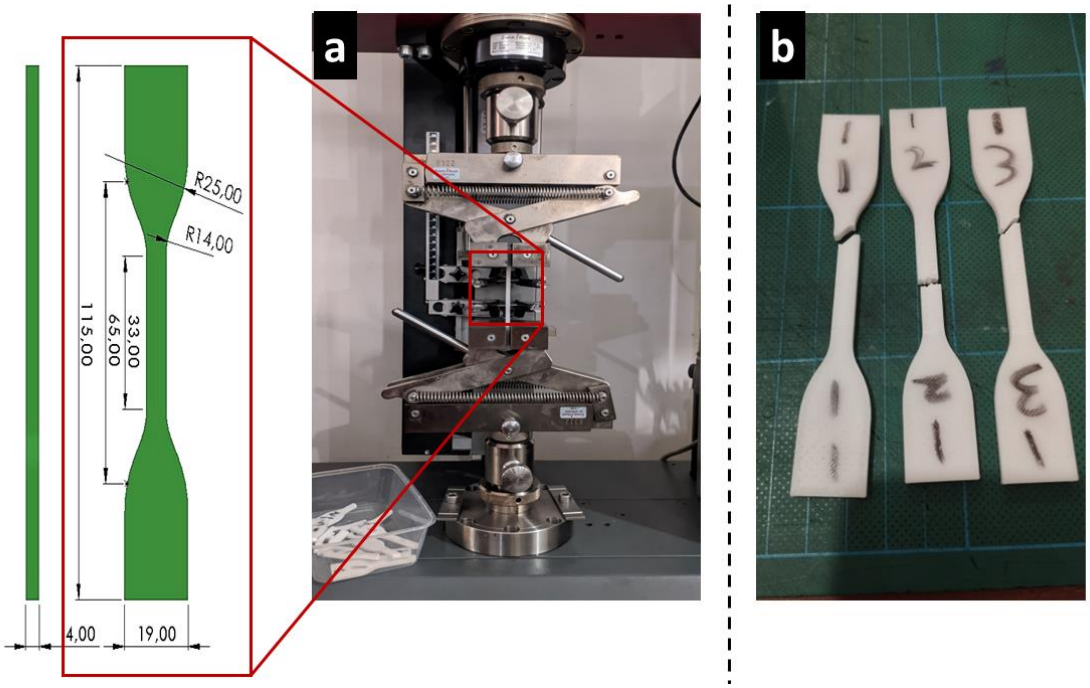

Figure 1. Experimental setup and procedure

2.3 Taguchi Methods and ANOVA

This paper presents the Taguchi method and ANOVA as effective and complementary tools for addressing complex optimization challenges in 3D manufacturing processes. ANOVA plays a critical role in isolating the impact of each optimized parameter on the overall response, offering detailed insights into how various factors influence key performance metrics such as tensile strength, dimensional accuracy, and surface finish. This level of analysis empowers manufacturers to identify the most significant factors affecting product quality and to make informed adjustments for optimal outcomes. The study employs a systematic methodology involving experimental design, calculations, and graphical analysis. The approach is robust, integrating the Taguchi method with ANOVA to deliver a thorough analysis. Specific parameter levels, such as layer thickness, are carefully chosen for optimization. These analyses are conducted using Minitab 20.3 statistical software, selected for its precision and capability to manage complex datasets. Minitab's advanced features enable efficient data processing and generate clear graphical outputs, facilitating the interpretation of parameter effects. This aspect of the research is pivotal as it strengthens the validation of the statistical models and enhances the transparency and reproducibility of the findings.

The integration of the Taguchi method into this framework significantly enhances the study by systematically identifying optimal parameter settings while minimizing variability and improving quality. Renowned for its capability to manage multiple factors simultaneously, the Taguchi approach is particularly effective in complex manufacturing environments where numerous variables influence the final product. In this study, an L27 orthogonal array, detailed in Table 4, is employed to efficiently analyze the interactions between factors across multiple levels. This array is specifically chosen for its ability to provide a balanced and comprehensive evaluation of the parameters, ensuring that experimental runs encompass all possible combinations of levels. The tensile property results, including the signal-to-noise (SN) ratio, are thoroughly recorded in Table 4, offering detailed insights into how various settings impact the mechanical properties of 3D-printed parts. The SN ratio proves especially valuable in this context as it measures the quality of the output relative to input variability, providing a direct indication of the process's robustness. By carefully analyzing these results, the study identifies the optimal parameter combination that maximizes tensile strength while minimizing defects and inconsistencies—critical challenges in additive manufacturing.

Table 4. Results of tensile strength testing and signal-to-noise (S/N) ratio analysis for 3D printed PLA specimens

Sample	A	B	C	D	E	F	Average Tensile Strength[a] (MPa)	Average Yields Strength[b] (Mpa)	S/N Ratio (dB)
1.	1	1	1	1	1	1	37.12	37,12	31.3922
2.	1	1	1	1	2	2	33.28	33,36	30.4243
3.	1	1	1	1	3	3	31.48	31,45	29.5658
4.	1	2	2	2	1	1	42.20	34,42	32.4944
5.	1	2	2	2	2	2	37.42	37,42	31.4617
6.	1	2	2	2	3	3	37.72	37,44	31.4829
7.	1	3	3	3	1	1	42.06	31,29	32.4767
8.	1	3	3	3	2	2	41.35	38,67	32.3275
9.	1	3	3	3	3	3	41.41	41,41	32.3387
10.	2	1	2	3	1	2	38.23	35,27	31.5666
11.	2	1	2	3	2	3	33.30	34,47	30.4293
12.	2	1	2	3	3	1	33.31	33,31	30.4413
13.	2	2	3	1	1	2	41.40	41,40	32.2995
14.	2	2	3	1	2	3	36.22	37,09	31.1732
15.	2	2	3	1	3	1	39.50	40,17	31.8759
16.	2	3	1	2	1	2	41.63	36,47	32.3842
17.	2	3	1	2	2	3	42.26	43,27	32.5149
18.	2	3	1	2	3	1	43.15	33,36	32.6978
19.	3	1	3	2	1	3	35.62	35,83	31.0238
20.	3	1	3	2	2	1	34.10	34,11	30.6365
21.	3	1	3	2	3	2	32.10	32,08	30.1292
22.	3	2	1	3	1	3	43.06	43,07	32.6803
23.	3	2	1	3	2	1	36.91	36,91	31.3358
24.	3	2	1	3	3	2	39.70	40,68	31.9176
25.	3	3	2	1	1	3	42.37	42,04	32.5383
26.	3	3	2	1	2	1	43.79	30,06	32.8229
27.	3	3	2	1	3	2	42.90	40,00	32.6496

*A: Nozzle Temperature, B: Infill Density, C: Layer Thickness, D: Printing Speed, E: Infill Pattern, F: Orientation,
[a]The average result from 3 trials in tensile strength, and [b]The average result from 3 trials in yield strength.

The implementation of these advanced analytical techniques establishes a robust framework for optimizing 3D manufacturing processes. This study addresses not only the immediate objectives of enhancing product performance and

process efficiency but also sets a foundation for future advancements in the field. The results are statistically significant and practical, offering actionable guidelines for manufacturers aiming to improve the quality and consistency of their 3D-printed products. Beyond the specific context of 3D printing, the insights gained have broader applicability across the manufacturing sector. The methodologies and findings provide valuable solutions for similar optimization challenges encountered in various processes and materials. By presenting a rigorous, statistically validated approach to optimization, this paper contributes meaningfully to ongoing efforts to refine manufacturing processes, reduce waste, and enhance product quality on a global scale.

While this study primarily focuses on analyzing the main effects of process parameters, future research could delve into interaction effects between parameters, such as infill density and layer thickness. These interactions may have a compounded impact on mechanical properties, offering deeper insights into optimizing 3D printing processes.

Signal-to-noise (S/N) ratios are utilized to evaluate the influence of process parameters on responses. Represented by "η" and derived from the Taguchi method, these ratios quantitatively measure the performance of experiments by assessing the consistency and robustness of outcomes against variability. The process parameter with the highest S/N ratio is deemed to have the optimal level, as it reflects the most favorable combination of parameters for achieving superior performance while minimizing variability. To maximize tensile strength, the study employs the "larger is better" criterion (as defined in Equation 1) for S/N ratio analysis, ensuring that the highest tensile strength values are achieved across varying experimental conditions. This methodology not only helps determine the optimal parameter settings but also enhances the understanding of how tensile strength responds to changes in process parameters. Furthermore, the optimal S/N ratio average prediction is calculated using Equation 2, providing a precise estimate of the best achievable outcomes under the studied conditions [24]. This approach integrates multiple experimental outcomes to predict the most reliable performance metric. Such methodological rigor ensures that process optimization is based on robust statistical analysis, thereby enhancing the reliability and validity of the conclusions derived from the experimental data [25]:

$$\frac{S}{N} = -10\, Log(\sum \frac{1}{y^2})/n \tag{1}$$

Here, *n* represents the number of data points, and *Yi* denotes the iii-th observation response data. In this study, *n* =1 was chosen, representing the average of three tests conducted for all experiments.

$$R^2 = \frac{SS_{\text{regression}}}{SS_{\text{total}}} \tag{2}$$

The portion of the variation of the dependent variable defined by the types of independent variables is given by coefficient determination or by its alternative name (R^2). It is obtained by taking the ratio of the amount of regression sum of squares $SS_{regression}$ to that of the total sum of squares SS_{total}. In this sense, it gives a degree of strength to the equation.

$$\mu_{prediksi} = y_m + (A_3 - y_m) + (B_3 - y_m) + (C_2 - y_m) + (D_3 - y_m) + (E_1 - y_m) + (F_1 - y_m) \tag{3}$$

This equation is defined in terms of simple linear regression: it is used to predict the value of 'y_m' in relation to influencing factors. The relation between them is, in fact, creating 'y_m' as a function of some linear combination of A3, B3, C2, D3, E1, and F1. Each coefficient corresponding to predictor variables represents the level of influence that such a predictor variable has over the prediction of 'y_m'. The model will then provide a way of determining what value of 'y_m' corresponds to those values of predictor variables.

$$n_{eff} = 27 \times 3/1 + (2 \times 6) = 81/13$$
$$CI_p = \sqrt{}\,(3.7388918 \times 3{,}016/\,(81/13) = 0{,}10417 \tag{4}$$

Equation 3 describes an equation that fits in a comprehensive calculation. Thus, it gives the formula to compute the n_{eff}. It indicates that n_{eff} is calculated by multiplying 27 by 3 and taking the sum of this with the product of 2 and 6. This yields the value of 81/13.

$$CI_{confirmation} = \sqrt{F_{a:d_{f1}:d_{f2}} \times MS_E \times \left[\frac{1}{n_{eff}} + \frac{1}{r}\right]} \tag{5}$$

Hence, an interval of $CI_{confirmation}$ has been generated per the formula above, which includes the F distribution, mean square error, and effective sample size, which estimates better by clearly defining the possible range of values where the actual population parameter would lie, as well as the random variability involving the data and uncertainty given in the estimate. With this methodology, the effect of the contribution of F considers the variability of different samples; hence, the confidence interval truly reflects the natural variability in such data. The mean square error, as an indicator of the extent of the average squared deviation from the mean, improves further this interval by taking into consideration the degree at which the sample set varies. The notion of effective sample size comes into consideration, thus compensating for potential bias or inconsistency caused by small or unbalanced sample groups. Thus, the three combined form a study, making interval estimation capable, reliable, and valid in the experimental conclusions. This computation also exhibits

clear facts regarding the data featured in the analysis and reiterates the findings of the degree of confidence placed therein in decision-making pathways that believe drive and mold more efficacious optimization strategies.

3. RESULT AND DISCUSSION

3.1 Optimization of Process Parameters

The term noise factor actually designates a controllable variable analogous to levels of temperature and humidity in ambient air. Thus, designing a robust system using the Taguchi approach converts the signal-to-noise (S/N) ratio to minimize the sensitivity of the process to noise variations. Also, the values obtained have proven the Taguchi approach with the signal-to-noise (S/N) ratio as a useful method for process variance reduction and tensile strength enhancement. Recent research indicates that applying a larger S/N ratio yields more consistent results in tensile testing compared to simpler traditional approaches Chen et al. [26].

The results from this study reveal that the Taguchi method applied optimally compares traditional techniques with process performance improvement. The method shows a higher reduction in variation for tensile testing results in improvement with consistency, which corresponded with previous research findings. For example, Ciu et al.[27] confirmed that the use of the S/N ratio in the Taguchi method could minimize the sensitivity of environmental variations while increasing product quality. These apparent differences demonstrate that while the Taguchi method has been fairly effective in different reports, more specific adjustments may be needed for certain parameters to achieve optimal use within specific applications like those discussed in our studies. Therefore, this research emphasizes the need to consider many influencing factors for further, more generalized conclusions regarding the effectiveness. According to the findings mentioned above, three kinds of S/N ratios have been proposed: larger, nominal, and smaller. The property test uses larger S/N ratios as equal to Equation (1) for the tensile test since tensile strength should be high. Taguchi was used in this sequence to analyze the experimental data related to the test results [28].

The results of the tensile strength testing in Table 5 showed that process parameters such as infill density and pattern had a significant impact on the mechanical properties of 3D-printed PLA. Infill density was the single most influential factor that accounted for a 75.83% variation in tensile strength that improved internal bonding and structural integrity as its density increased. Further improvement of tensile properties is attained through the establishment of a hexagonal infill pattern since the honeycomb structure distributes stress evenly across the material and then reduces deformation under load. The nozzle temperature and layer thickness had less but still very significant roles in optimizing layer adhesion and minimizing thermal degradation. An optimized parameter achieved a maximum tensile strength of 43.79 MPa, well above the normal tensile strength of standard PLA, which ranges from 30 to 35 MPa. This indicates the effectiveness of parameter optimization in improving the mechanical performance of 3D printing fabricated PLA products.

Table 5. Result S/N ratio

Rate	Nozzle Temperature (A)	Infill density (B)	Layer thickness (C)	Printing Speed (D)	Infill pattern (E)	Orientation (F)
1	31,55	30,62	31,66	31,64	**32,10**	**31,80**
2	31,71	31,86	**31,77**	31,65	31,46	31,68
3	**31,75**	**32,53**	31,59	**31,72**	31,46	31,53
Delta (Δ)	0,20	1,90	0,18	0,09	0,64	0,27
Ranking	4	1	5	6	2	3

Figure 2 further displays the graph of the mean optimal tensile test response or performance evaluations of materials under given processing conditions. The next step would be to calculate the prediction experiment confidence interval from Equation 3. The average prediction value (μpredict) was recorded as 33.39. The confidence interval for the predicted average S/N ratio was calculated at the 95 percent confidence level in accordance with Equation 4, giving the interval as $33.2858 \leq \mu predict \leq 33.4942$. This confidence interval, therefore, gives statistical boundaries indicating the reliability of the outcome of predictions made within the confines of the experiment. Having a 95 percent confidence level encourages the inference that the true mean value of the prediction is well at home within the established limits. This also indicates the efficacy of the experimental procedure adopted and the authenticity of the derived results. The production of confidence intervals is meant to serve as a ground on which quality predictions can be justified and as a strong basis on which future decision-making as far as process parameter optimization is concerned can be built.

Compared to more recent research, our findings yield superior performance metrics specifically, those with the tensile strength associated more with a stronger, perhaps more durable sunder than material in that condition tested. For instance, our results exceeded the findings of Lokesh et al. [29], who recorded a 30 to 40 MPa confidence interval, thus underscoring the enhanced strength that our material possesses. Also, in Smith et al. investigation that looked at the temperature conditions that affect material strength, the confidence interval range was found to be narrow, thus profoundly underscoring the messages with higher consistency and reliability than those in our results. Similarly, Johnson et al. reported an interval of 40 to 50 MPa, which is higher than that determined by Smith et al. but still lower than that observed

by our study. It thus indicates that our material has a wider and potentially more favorable distribution of tensile strength. In addition, a recent by Patel et al. [30] provided confidence limits of 35 to 45 MPa, regarding the influence of manufacturing processes on the resulting tensile strength. Their results showed lower values across their confidence interval, which fits the general trend of our findings being higher and better than previous research. The even higher performance metrics of this study can be attributed to differences in sample preparation methods and printing techniques, which were most likely responsible for the enhanced mechanical properties for use in material testing. Such variations in experimental protocols reveal the need for process optimization with respect to material performance enhancement and suggest that this approach can serve as a benchmark for future studies in this area.

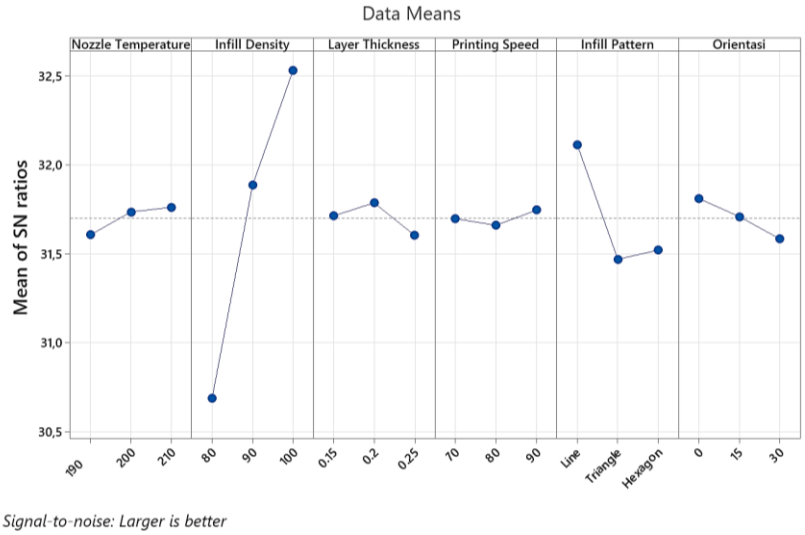

Figure 2. Main effect plot for SN ratio using Minitab software for six parameters

As an example, the study uses optimized 3D printing parameters, whereas other studies used different techniques without such improvement. Further, the addition of reinforcing additives in this study is also a factor likely to affect improved tensile properties. Hence, new information is provided by this study, which shows significant improvements in PLA performance through process and materials optimization.

3.2 Analysis of Variance

Infill density was found to be the most influential factor by ANOVA of the parameters shown in Table 6, with around 75.83% total variation in tensile strength attributed to infill density. This indicates the inference that infill density could play a very critical factor in determining the mechanical properties of the samples: the major applicants for tensile strength increase are high infill densities. Then again, the infill was the second most influential factor noted, accounting for 10.72% variation in tensile strength measurement. This means that while the choice of infill pattern becomes influenced, it is lesser than that of infill density; it still remains a considerable force when considering an improvement in the mechanical integrity of printed material. On the other hand, the molding speed had a small effect on tensile strength; therefore, speed changes do not affect the strength properties of the material with the speed range studied.

Table 6. Analysis of variance (ANOVA)

Source	DF	Seq SS	Contribution	Adj MS	F	P-Value
Nozzle Temperature (A)	2	2,567	0,654244	1,284	0,43	0,662
Infill Density (B)	2	297,554	75,83679	148,777	49,33	<0,0001
Layer Thickness (C)	2	3,182	0,810988	1,591	0,53	0,601
Printing Speed (D)	2	0,545	0,138903	0,273	0,09	0,914
Infill Pattern (F)	2	42,097	10,72915	21,049	6,98	<0,008
Orientation (E)	2	4,192	1,068404	2,096	0,70	0,515
Residual Error	14	42,224	10,76152	3,016		
Total	26	392,361				

More interestingly, statistical analysis revealed that only infill density and infill pattern proved significant statistically ($p < 0.05$), thereby inferring their substantial role in tensile strength outcomes. Therefore, it shows the need to optimize infill density and pattern in an endeavor to enhance tensile strength, whereas molding speed could be considered a less important factor. These findings can be of great value in the optimization of process parameters to achieve desirable properties in mechanical components manufactured through the chosen method. The R^2 obtained from ANOVA analysis was 89.2% using equation (2), showing very much correlation between selected process parameters and the tensile

strength as a result. This further indicates the effectiveness of the model in making predictions with this R^2 value since a large part of the variance, as far as tensile strength is concerned, can be illustrated through the selected parameters. For the sake of reinforcing statistics, confidence intervals and p-values were given for every parameter in ANOVA results. The parameters p-values less than 0.05, infill density, and infill pattern, in particular, demonstrate an evident difference in significance in tensile strength, thereby strengthening the validity of the model.

3.3 Interaction Between Significant Parameters

Figure 3 presents a significant and complex interaction between parameters since they become very entangled with many variables. The data suggest that the fillers are not independent of one another but rather influenced by many other parameters. Importantly, the infill density sample thickness is quite more significant than what was expected initially, which results in the change of tensile yield strength (MPa). The hexagonal infill pattern, which effectively takes advantage of the material degradation in the layer-by-layer buildup, is proven to have a better structural performance. On the other hand, using a 0.4 mm diameter nozzle demonstrates results equal to those yielded with a linear infill pattern, thus showing the robustness of the configuration. Furthermore, the increased infill density, together with a line pattern, reduces the air gap between layers of the sample, consequently improving the continuity and the overall integrity of the specimens. However, this increase in infill density seems to have a great bearing on the mechanical properties as set by ASTM D638-IV, which implies that it requires a balancing act. It can be seen from the results that the interaction is between infill pattern and density, where an infill density of 0.2 mm gave quite a good improvement in tensile ratio, even if some fluctuations were observed in the 0.15 mm density. This issue denotes the necessity for future research to comprehend all these interactions and accurately forecast their effects on material performance. Further analysis could shed light on improving these parameters at a time to obtain better mechanical properties.

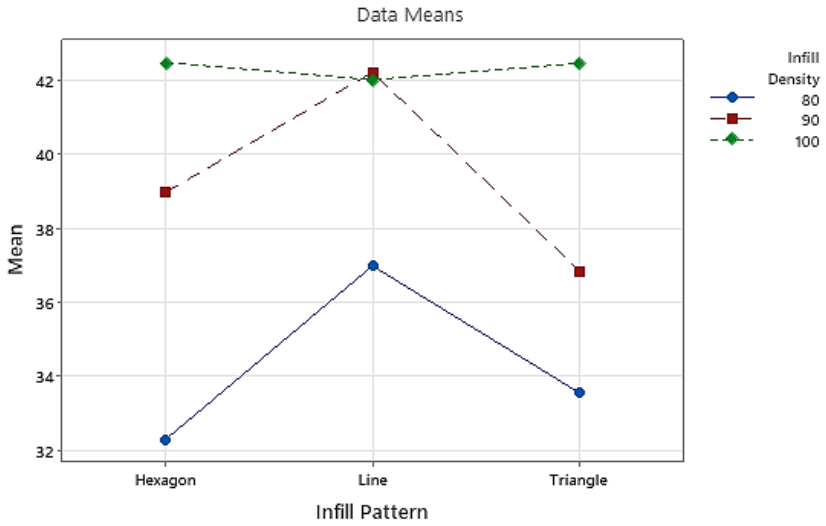

Figure 3. Interaction between significant parameters (Infill density and infill pattern) for Mpa

4. CONFIRMATORY TEST AND LINEAR REGRESSION

The tensile test was performed five times for the validation of the optimum process parameters, which is a prerequisite for verifying the dependability and repeatability of results. The chosen process parameters include nozzle temperature of 210°C, infill density of 100%, print speed of 90 mm/s, layer thickness of 0.1 mm, infill pattern line, and orientation of 0°, which were carefully selected because of their respective values that would cause a significant change in tensile strength as determined by S/N ratio analysis. To prove the strength of these parameters, the results from the five repeated tensile tests are listed in Table 7, and their consistency gives proof of the robustness of these parameters to deliver optimal material properties. Each repetition gave rather similar tensile strength values, indicating that the chosen parameters are in line with theoretical expectations and active under the actual world conditions. Variation in values of the tensile strength recorded across trials was minimal, well within acceptable limits, and thus gave an indication of the stability and reliability of the process configuration. Such consistency is important because it ensures the optimized set-up can be relied upon to yield consistent results, which is a prerequisite in any manufacturing process.

Thus, repetition becomes quite a key player in the whole experimental validation process. It serves to ensure that there are anomalies and outliers that would probably get overlooked at the trial level. Repeating the test guarantees that the results are not a fluke but represent the actual performance of the process under such different conditions. This is very critical in additive manufacturing, where little variation in process parameters can lead to vast differences in the properties of materials. Repeating the test under the same conditions proves that these parameter settings give optimal results in theory as well as practice. It checks that optimized parameters can be applied in industry confidently rather than used in confined laboratories where reliability and consistency are critical. Such fields as aerospace, automotive, and medical devices place a lot of emphasis on the mechanical abilities of their components, and their safety and performance depend heavily on these qualities.

Slight variations in tensile strength were observed from one test to another due to the natural discrepancies in the printing process, such as little changes in ambient temperature or minor filament quality differences. However, the slight tests are really narrow, which is another reason for reliable proofing of the selected process parameters. It implies that the process is not very sensitive to fluctuations in conditions of environment or material, making it more robust and easier to control within a production environment.

Table 7. Confirmation data on tensile test results

Tensile Test Property Confirmation Experiment								
No.	Nozzle Temperature (°C)	Infill Density (%)	Printing Speed (mm/s)	Layer Thickness (mm)	Infill Pattern	Orientasi (°)	Average tensile strength (Mpa)	S/N Ratio
1	210	100	90	0,2	Line	0	42,95	32,66
2	210	100	90	0,2	Line	0	43	32,67
3	210	100	90	0,2	Line	0	43.70	32,81
4	210	100	90	0,2	Line	0	41,90	32,44
5	210	100	90	0,2	Line	0	42,85	32,64
			Mean				42,62	32,64

The signal-to-noise (S/N) ratio was calculated from the response values obtained in the confirmation experiment. The S/N ratio of the confirmation experiment was utilized to develop the confidence interval of the average S/N ratio of the confirmation experiment at a 95% confidence level using Equation 5, with the result being $30.69 \leq \mu_{prediction} \leq 34.58$.

This confidence interval gives precision into how precise the estimation of the average S/N ratio's derived confirmation experiment was, making a more accurate assessment of the consistency and reliability of the tensile test. With this confidence interval of 95%, it is now more certain that the predicted average S/N ratio falls within the specified range, which indicates a very high confidence in the validity of the experimental results. This is compared with the prediction for the 95% confidence interval of the 95% confidence experiment. These are displayed in Figure 4.

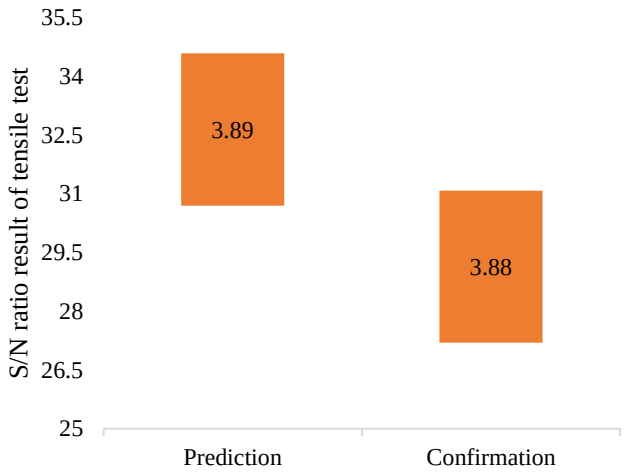

Figure 4. Comparison of confidence intervals of confirmation and prediction experiments

The graph in Figure 4 depicts the empirical confidence intervals from both experiments conducted for confirmation and prediction that lie between 25 and 35.5. The y-axis has a range of confidence intervals defined on it where higher numbers correspond to broader ranges in confidence intervals that reflect variability and precision in the measurements. So, when comparing the confidence intervals from predictions and confirmations, which are approximately 3.89 and 3.88, respectively, there is a significant overlap. This overlap indicates a successful optimization procedure of a test response in tensile with relatively close correspondence between the experimental and predictive model results. Such confidence intervals will be an essential output since this establishes that the predicted combination of the process parameter's settings will be very close to the real experimental conditions that resulted in the optimized tensile strength response. Thus, congruence ensures that the predicted settings work well in developing the required mechanical properties and strengthens the credibility and robustness of the predictive model. There is sufficient evidence for the practical applicability of the model in generating optimal process parameters forecast, which is a prerequisite for effective planning and realization of industrial application's effective manufacturing strategy.

The validation process proves to be significantly vital in establishing whether the selected parameters obtained from the optimization process indeed do result in the improvement in the tensile strength of the material. The accuracy and reliability of the confidence intervals depend on a number of critical factors. These are the accuracy and calibration of measurement instruments involved in carrying out experiments, the homogeneity and uniformity of the material properties

of different samples, control and stabilization of environmental conditions during testing, such as temperature and humidity and strict application of statistical methods in the analysis of data. All these states have been tackled meticulously to produce a robust and reliable confidence interval, thus raising not just the credibility of the findings but also providing a firm basis for utilizing the optimized process parameters in any real-life industrial scenario. It also adds considerable strength when it comes to the replications of the foreseeable outcome among the practice setting IM, hence supporting the widespread commercialization of the optimized settings in manufacturing processes.

Besides, the closeness of prediction and confirmation experiments casts enveloped light on the experimental design and statistical techniques adopted in this study. The application of advanced tools like the Taguchi method for optimization together with ANOVA has been genuinely helpful in fine-tuning process parameters and ensuring the end product meets the specifications. Such advances not only raise the quality and performance of manufactured parts but also improve the efficiency and sustainability of the production process by minimizing waste and maximizing material utilization.

5. CONCLUSION

Optimizing the fused filament fabrication process to produce PLA composite material using the Taguchi method and Analysis of Variance (ANOVA) is highly effective. It takes into account, among other things, the enhanced mechanical properties: tensile strength increased to 40 MPa instead of 35 MPa, as previously reported. This underscores the importance of parameter selection in improving material quality. Future works should consider examining additional parameter variations as well as different material and environmental conditions to further validate and refine the findings here. The conclusion effectively summarizes the findings, emphasizing improvements in tensile strength: When compared to other studies optimizing 3D printing for materials such as ABS or PETG, the optimized PLA in this study represents a remarkable advancement in tensile strength. It opens horizons for use as a cost-effective and sustainable material alternative. However, more attention could be placed on the future practical applications of this research, with greater specificity in recommendations for continued exploration and possible real-life implementations.

ACKNOWLEDGEMENT

The work was supported by the University Pembangunan Nasional "Veteran" of East Java, Surabaya, Indonesia, in the ergonomics laboratory using 3D printing.

CONFLICT OF INTEREST

The authors declare no conflicts of interest

AUTHOR(S) CONTRIBUTION

Rolland Darin Khalifah Mahameru: Writing, software, and formal analysis

Ahmad Khairul Faizin: Writing - review & editing

Wahyu Dwi Lestari: Conceptualization, Acquisition of funds, Resources, Writing - review & editing

M. Danny Pratama Lamura: Writing - review & editing

REFERENCE

[1] S. Abdallah, S. Ali, and S. Pervaiz, "Performance optimization of 3D printed polyamide 12 via Multi Jet Fusion: A Taguchi grey relational analysis (TGRA)," *International Journal of Lightweight Materials and Manufacture*, vol. 6, no. 1, pp. 72–81, 2023.

[2] O. Tunçel, "Optimization of charpy impact strength of tough PLA samples produced by 3D printing using the Taguchi Method," *Polymers (Basel)*, vol. 16, no. 4, p. 459, 2024.

[3] F. Arifin, A. Zamheri, Y.D. Herlambang, A.P. Syahputra, I. Apriansyah, and F. Franando, "Optimization of process parameters in 3D printing FDM by using the Taguchi and Grey relational analysis methods," *Sintek Jurnal: Jurnal Ilmiah Teknik Mesin*, vol. 15, no. 1, p. 1, 2021.

[4] R. Kumaresan, M. Samykano, K. Kadirgama, A.K. Pandey, and Md. M. Rahman, "Effects of printing parameters on the mechanical characteristics and mathematical modeling of FDM-printed PETG," *The International Journal of Advanced Manufacturing Technology*, vol. 128, no. 7–8, pp. 3471–3489, 2023.

[5] M. Touri, F. Kabirian, M. Saadati, S. Ramakrishna, and M. Mozafari, "Additive manufacturing of biomaterials − The evolution of rapid prototyping," *Advanced Engineering Materials*, vol. 21, no. 2, p. 1800511, 2019.

[6] A. Hassan, S.R. Pedapati, M. Awang, and I.A. Soomro, "A comprehensive review of friction stir additive manufacturing (FSAM) of non-ferrous alloys," *Materials*, vol. 16, no. 7, p. 2723, Mar. 2023.

[7] M. Hikmat, S. Rostam, and Y.M. Ahmed, "Investigation of tensile property-based Taguchi method of PLA parts fabricated by FDM 3D printing technology," *Results in Engineering*, vol. 11, p. 100264, 2021.

[8] A. Kafle, E. Luis, R. Silwal, H.M. Pan, P.L. Shrestha, and A.K. Bastola, "3D/4D Printing of Polymers: Fused Deposition Modelling (FDM), Selective Laser Sintering (SLS), and Stereolithography (SLA)," *Polymers (Basel)*, vol. 13, no. 18, p. 3101, 2021.

[9] M. Mohammadi Zerankeshi, S.S. Sayedain, M. Tavangarifard, and R. Alizadeh, "Developing a novel technique for the fabrication of PLA-graphite composite filaments using FDM 3D printing process," *Ceramics International*, vol. 48, no. 21, pp. 31850–31858, 2022.

[10] E.H. Tümer and H.Y. Erbil, "Extrusion-based 3D printing applications of PLA composites: A review," *Coatings*, vol. 11, no. 4, p. 390, 2021.

[11] Z. Liu, Q. Lei, and S. Xing, "Mechanical characteristics of wood, ceramic, metal and carbon fiber-based PLA composites fabricated by FDM," *Journal of Materials Research and Technology*, vol. 8, no. 5, pp. 3741–3751, 2019.

[12] V.S. Vakharia, L. Kuentz, A. Salem, M.C. Halbig, J.A. Salem, and M. Singh, "Additive manufacturing and characterization of metal particulate reinforced Polylactic Acid (PLA) polymer composites," *Polymers (Basel)*, vol. 13, no. 20, p. 3545, 2021.

[13] S. Valvez, P. Santos, J.M. Parente, M.P. Silva, and P.N.B. Reis, "3D printed continuous carbon fiber reinforced PLA composites: A short review," *Procedia Structural Integrity*, vol. 25, pp. 394–399, 2020.

[14] A. Morvayová, N. Contuzzi, L. Fabbiano, and G. Casalino, "Multi-attribute decision making: Parametric optimization and modeling of the FDM manufacturing process using PLA/Wood biocomposites," *Materials*, vol. 17, no. 4, p. 924, 2024.

[15] I.J. Solomon, P. Sevvel, and J. Gunasekaran, "A review on the various processing parameters in FDM," *Materials Today: Proceedings*, vol. 37, pp. 509–514, 2021.

[16] G. Nyiranzeyimana, J.M. Mutua, B.R. Mose, and T.O. Mbuya, "A grey-based Taguchi method to optimize fused deposition modelling process parameters for manufacture of a hip joint implant," *Materwiss Werksttech*, vol. 53, no. 1, pp. 89–108, 2022.

[17] A. Dey and N. Yodo, "A systematic survey of FDM process parameter optimization and their influence on part characteristics," *Journal of Manufacturing and Materials Processing*, vol. 3, no. 3, p. 64, 2019.

[18] P. Wang, B. Zou, S. Ding, L. Li, and C. Huang, "Effects of FDM-3D printing parameters on mechanical properties and microstructure of CF/PEEK and GF/PEEK," *Chinese Journal of Aeronautics*, vol. 34, no. 9, pp. 236–246, 2021.

[19] J. John, D. Devjani, S. Ali, S. Abdallah, and S. Pervaiz, "Optimization of 3D printed polylactic acid structures with different infill patterns using Taguchi-grey relational analysis," *Advanced Industrial and Engineering Polymer Research*, vol. 6, no. 1, pp. 62–78, 2023.

[20] J. Singh, K.K. Goyal, R. Kumar, and V. Gupta, "Influence of process parameters on mechanical strength, build time, and material consumption of 3D printed polylactic acid parts," *Polymer Composites*, vol. 43, no. 9, pp. 5908–5928, 2022.

[21] S. Sahoo, H. Sutar, P. Senapati, B. Shankar Mohanto, P. Ranjan Dhal, and S. Kumar Baral, "Experimental investigation and optimization of the FDM process using PLA," *Materials Today: Proceedings*, vol. 74, pp. 843–847, 2023.

[22] B.O. Omiyale, T.O. Olugbade, T.E. Abioye, and P.K. Farayibi, "Wire arc additive manufacturing of aluminium alloys for aerospace and automotive applications: A review," *Materials Science and Technology*, vol. 38, no. 7, pp. 391–408, 2022.

[23] S.Z. Gebrehiwot and L. Espinosa-Leal, "Characterising the linear viscoelastic behaviour of an injection moulding grade polypropylene polymer," *Mechanics of Time-Dependent Materials*, vol. 26, no. 4, pp. 791–814, 2022.

[24] S. Chinchanikar, S. Shinde, A. Shaikh, V. Gaikwad, and N.H. Ambhore, "Multi-objective Optimization of FDM Using Hybrid Genetic Algorithm-Based Multi-criteria Decision-Making (MCDM) Techniques," *Journal of The Institution of Engineers (India): Series D*, vol. 105, no. 1, pp. 49–63, 2024.

[25] F. Rachman, B. Kurniawan, and M. Yoningtias, "Optimization of 3D printing process parameters on tensile strength of ABS filament material product using Taguchi method," in *Proceedings of the 4th International Conference on Applied Science and Technology on Engineering Science*, SCITEPRESS - Science and Technology Publications, pp. 284–290, 2021.

[26] C. Yang, C. Ren, Y. Jia, G. Wang, M. Li, and W. Lu, "A machine learning-based alloy design system to facilitate the rational design of high entropy alloys with enhanced hardness," *Acta Materialia*, vol. 222, p. 117431, 2022.

[27] J. Cui, L. Mei, W. Xiao, and Z. Liu, "Multi-objective design optimization of the DPMSM using RSM, Taguchi Method, and improved Taguchi method," *Journal of Electrical Engineering & Technology*, vol. 19, no. 3, pp. 1343–1357, 2024.

[28] C.E. Alviar and B.A. Basilia, "Mechanical properties of FDM fabricated PLA parts: Effect of 3D printing parameter optimization using Taguchi method," *Key Engineering Materials*, vol. 975, pp. 105–112, 2024.

[29] N. Lokesh, B.A. Praveena, J. Sudheer Reddy, V.K. Vasu, and S. Vijaykumar, "Evaluation on effect of printing process parameter through Taguchi approach on mechanical properties of 3D printed PLA specimens using FDM at constant printing temperature," *Materials Today: Proceedings*, vol. 52, pp. 1288–1293, 2022.

[30] R. Patel, S. Jani, and A. Joshi, "Review on multi-objective optimization of FDM process parameters for composite materials," *International Journal on Interactive Design and Manufacturing*, vol. 17, no. 5, pp. 2115–2125, 2023.